## *Rapid assessment of beta dose variation inside cobbles, and implications for rock luminescence dating*

Ou, X.j.; Roberts, H.m.; Duller, G.a.t.

*Published in:*
Quaternary Geochronology

*DOI:*
10.1016/j.quageo.2022.101349

*Publication date:*
2022

*Citation for published version (APA):*
Ou, X. J., Roberts, H. M., & Duller, G. A. T. (2022). Rapid assessment of beta dose variation inside cobbles, and implications for rock luminescence dating. *Quaternary Geochronology*, [101349]. https://doi.org/10.1016/j.quageo.2022.101349

Quaternary Geochronology 72 (2022) 101349

Contents lists available at ScienceDirect

Quaternary Geochronology

journal homepage: www.elsevier.com/locate/quageo

# Rapid assessment of beta dose variation inside cobbles, and implications for rock luminescence dating

X.J. Ou [a,b,*], H.M. Roberts [b], G.A.T. Duller [b]

[a] School of Geography and Tourism, Jiaying University, Meizhou, 514015, China
[b] Department of Geography and Earth Sciences, Aberystwyth University, Ceredigion, SY23 3DB, UK

ARTICLE INFO

*Keywords:*
Rock luminescence dating
Beta dose rate heterogeneity
Homogeneity
XRF
Beta counting

ABSTRACT

Variation in beta dose rate within rocks may impact the results of rock surface luminescence dating, for both the burial age of cobbles and exposure age of rock surfaces. Current methods of rock surface luminescence dating assume that radionuclides are homogeneously distributed inside rocks. In this study, two rapid methods based on beta counting and on a portable XRF instrument were developed to measure the radioactivity of rock slices. These methods were applied to rock slices from four glaciofluvial granite cobbles that had previously been used for equivalent dose determination to test whether beta dose variation could be observed. Results from beta counting and K content from XRF show similar patterns and both vary along the depth profiles, but the magnitude of this variability is very different amongst the four cobbles. In rocks where the dose rate is highly variable, bleaching may not be the only source of variation of $L_n/T_n$ or equivalent dose ($D_e$) along the luminescence-depth profile of cobbles, and it may be necessary to measure the beta dose rate for every single slice to determine whether multiple bleaching events are recorded or variations in $D_e$ are due to dose rate heterogeneity.

## 1. Introduction

Rock surface luminescence dating has been applied increasingly in geoscience and archaeology in recent years for both determining exposure age (e.g. Brill et al., 2021; Lehmann et al., 2018; Liritzis, 2011; Luo et al., 2018; Sohbati et al., 2011, 2018) and burial age (e.g. Ageby et al., 2021; al Khasawneh et al., 2019; Bailiff et al., 2021; Chiverrell et al., 2021; Feathers et al., 2019; Freiesleben et al., 2015; Gliganic et al., 2021; Ishii et al., 2022; Jenkins et al., 2018; Rades et al., 2018; Simkins et al., 2016; Sohbati et al., 2015; Souza et al., 2019) of rock surfaces and cobbles. However, previous age determination, curve fitting etc., was based on the assumption that radionuclides are homogenously distributed within each rock, and that variations in luminescence are due only to the history of bleaching and burial.

For rocks, the beta dose rate is often the major contribution to the total dose rate (Fang et al., 2018; Plachy and Sutton, 1982; Simkins et al., 2016) of slices used for dating, especially for granite cobbles, which are the main target material in recent rock surface luminescence dating studies. Rock surface luminescence exposure dating estimates the age by fitting Ln/Tn profile into the rocks, assuming a consistent dose rate contribution from the rock itself (e.g. Brill et al., 2021; Lehmann et al., 2018; Liritzis, 2011; Luo et al., 2018; Sohbati et al., 2011, 2018). If beta dose variation occurs it could have an impact on $L_n/T_n$, the shape of the luminescence-depth profile, and hence the exposure age of rock surfaces. Thus far, most published burial ages of cobbles (e.g. Ageby et al., 2021; al Khasawneh et al., 2019; Chiverrell et al., 2021; Feathers et al., 2019; Freiesleben et al., 2015; Gliganic et al., 2021; Ishii et al., 2022; Jenkins et al., 2018; Rades et al., 2018; Simkins et al., 2016; Sohbati et al., 2015; Souza et al., 2019) were also determined based on the assumption of homogeneous radionuclide distribution through the rock studied. With the exception of Feathers et al. (2019), who measured 3 rock slices, very little work has measured the beta dose rate for different rock slices. Variation of equivalent dose along the age-depth profile has been interpreted as being due to multiple phases of exposure and burial (e.g. Freiesleben et al., 2015; Jenkins et al., 2018; Rades et al., 2018; Sohbati et al., 2015), but such features may potentially also result from variation of dose rate within the rock. Therefore, the source of any variation of equivalent dose should be confirmed, and variability in dose rate ruled out as a cause, before identifying plateaus in the age-depth profiles as distinct deposition events.

Recent mapping of the minerals present in rocks (Fang et al., 2018; Sellwood et al., 2019) and modelling of dose rate distributions (Fang

* Corresponding author. School of Geography and Tourism, Jiaying University, Meizhou, 514015, China.
*E-mail address:* ouxianjiao@163.com (X.J. Ou).

https://doi.org/10.1016/j.quageo.2022.101349
Received 27 January 2022; Received in revised form 2 June 2022; Accepted 5 June 2022
Available online 11 June 2022

et al., 2018) showed that the assumption of homogeneous radionuclide distribution is not applicable to all rocks. Micro X-ray fluorescence (μXRF) spectroscopy (Sellwood et al., 2019) and energy dispersive spectroscopy (QEM-EDS) (Fang et al., 2018) have been used to map the distribution of minerals and different elements inside rocks. In situ LA-ICP-MS measurement (Fang et al., 2018) demonstrated that radionuclides, especially U and Th, are commonly unevenly distributed in rocks. This indicates that dose rate along the luminescence-depth profile may be heterogeneous, and it would seem likely that the degree of variation may vary considerably depending upon the rock.

However, mapping or modelling mineral or beta dose rate distributions in rocks is labour intensive and requires specialist equipment (e.g. μXRF, SEM, QEM-EDS, LA-ICP-MS). And there is still a lack of work to investigate beta dose variation along the luminescence-depth profile of dating rock samples. In this study, two rapid methods based on beta counting and on the use of a portable XRF instrument were investigated, to seek a practical way to assess the variability of beta dose rapidly using common laboratory equipment, either to allow preferential selection of those rocks with more homogeneous radionuclide distributions for dating, or to judge whether more detailed modelling is needed to assess the dose rate.

## 2. Materials and methods

Four glaciofluvial granite cobbles were collected from two sites in the United Kingdom associated with deglaciation of the last British-Irish Ice Sheet. Cobbles LL1D-01, LL1D-04 and LL1D-09 were collected from Lydiate Lane Quarry about 20 km north-east of Liverpool, while cobble WDL-02 was from Wood Lane Quarry about 30 km south of Chester on the Welsh/English border (Chiverrell et al., 2021). They were all obtained from gravel-dominated lithofacies. We also selected a piece of obsidian from the Big Obsidian Flow (BOF), Newberry, USA for comparison. This obsidian sample has previously been proposed as a geochemical standard because of its chemical uniformity (Laidley and McKay, 1971).

These cobbles were drilled using a bench-mounted pillar drill fitted with a water-cooled sintered diamond core bit to obtain cores ~7 mm in diameter and 20–30 mm long. Then the cores were cut into slices ~0.44 mm thick with exception of BOF slices (~0.38 mm thick), using a water-cooled low speed saw mounted with a 0.3 mm thick diamond wafer blade. The slices were cut with as uniform thickness as possible.

### 2.1. Beta counting measurements

Beta counting was conducted using a Risø Low-level beta GM-25-5 beta counter (Bøtter-Jensen and Mejdahl, 1988) to determine the total beta dose rate. For bulk sediment samples measured at Aberystwyth Luminescence Research Laboratory (ALRL), plastic pots ~ 25 mm in diameter and ~6 mm deep are normally packed full with powdered sample (~3 g mass), and then covered in a thin plastic film (cling film is the term used in the UK) that prevents spillage of the powder and absorbs alpha particles, but which does not attenuate the emitted beta particles. Pots are inserted into the counter so that the thin plastic film on the upper surface of each pot is close to the Geiger-Mueller detector. Beta activity is calculated by comparing the beta count rate from unknown samples with the count rate measured from samples of known beta activity. At ALRL the two standards used are powders of MgO and a Shap granite (beta activities of 0.0 and 5.99 Gy/ka). The instrument can simultaneously count 5 samples, and in routine use two positions contain the known-activity standards and the remaining three have samples of unknown activity, so that the calibration allows for short term fluctuations in counting efficiency. Results are also corrected for small variations in the sensitivity of each of the 5 counting positions. This approach has been in use at ALRL for more than 20 years.

For measuring the beta activity of rock slices (~0.44 mm thick and ~7 mm diameter), the plastic pots were turned upside down and slices were placed on top of the upturned pot with cling film used to hold them in place. The upturned pot was placed in the beta counter with the rock slice at the top, close to the Geiger-Mueller detector. Normally when using the beta counter one would have two known-activity standards with the same geometry as the unknown samples, but in this application that is hard to achieve (discussed in Section 4.1). Instead, we have used the packed-pots containing powdered MgO and Shap granite standards to calibrate each set of measurements and correct for short term fluctuations in counting efficiency. Section 3.1.3 describes how the count rate from rock slices measured alongside the powdered standards is converted into beta dose rate for each rock slice. Beta counting measurements took between 24 and 200 h for each set of three slices depending upon their size and beta count rate.

### 2.2. Reproducibility of beta counting rock slices

To assess the reproducibility of measurements on the beta counter, three rock slices from one glaciofluvial cobble (LL1D-01) were measured repeatedly using the procedure described above. Each slice was counted 23 times and between each measurement the beta pots were removed from the beta counter and the measurement position changed (position 1 went to position 2, 2 to 3, 3 to 4, 4 to 5 and position 5 went to position 1). This rotation of samples and standards is normal practice in ALRL. For each of the three rock slices, the mean and standard deviation of the beta count rate were calculated, and these used to determine the relative standard deviation (RSD). The RSD values for the three slices were 5.3%, 7.2% and 5.3%, giving an overall RSD of 5.9%. For each measurement a minimum of 2000 counts were acquired for each slice, implying an uncertainty of 2.2% due to counting statistics. The remaining scatter is most likely to result from the propagation of additional uncertainty during the correction for variations in the counting efficiency of each of the five positions.

### 2.3. Portable XRF K content measurements

Potassium (K) content was measured using a Thermo Niton XL3t GOLDD+ portable XRF, with an ~ 6 mm diameter X-ray beam. Samples were placed on silica to provide a simple background of known chemistry and ensure there was no contribution from the work surface below or around the sample. The measurements were performed with the XRF head flush with the surface of each sample. Samples were positioned as central to the XRF measurement window as possible. Each measurement was undertaken for a total of 35 s (the main range and low range were set as 5 s and 30 s, respectively).

### 2.4. Accuracy of portable XRF K content measurement

The accuracy of the portable XRF for measuring K content was tested using powdered standards such as NIST 70a, NIST 99a and MgO. In addition, a series of samples with independent geochemical determinations of K content were also measured; these include a loess from the USA (44ALRL-BH37), a loess from Belgium (Volkegem; De Corte et al., 2007), a beach sand from a recent laboratory inter-comparison (Murray et al., 2015), CTL05 and USGS-682-157 (Forman, personal communication), Shap granite (Sanderson, personal communication), and the Big Obsidian Flow, Newberry Caldera (Laidley and McKay, 1971; Higgins 1973; Pearce, personal communication). Comparison of the independent estimates of K and the value of K obtained from the portable XRF shows an excellent linear relationship, but with a small offset and a slope of 0.88 (Fig. 1); all K contents measured with the portable XRF in this paper have been corrected using the equation describing this relationship (shown in Fig. 1).

## 3. Challenges and correction of raw data

Measurement of the beta dose rate or the K content of rock slices

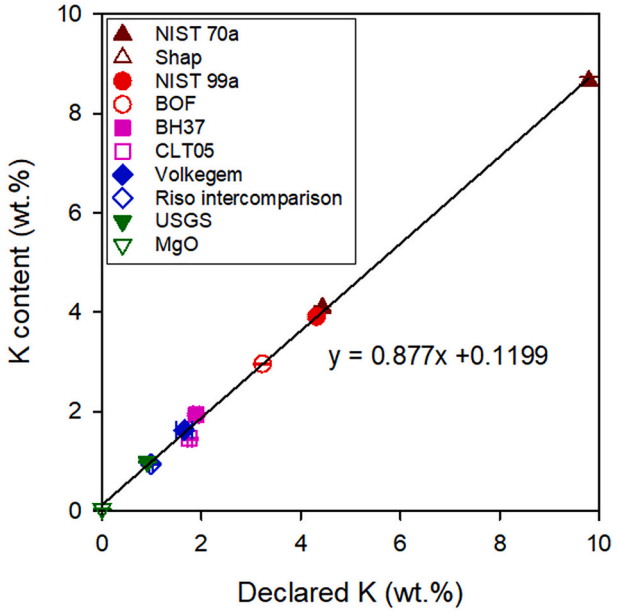


**Fig. 1.** Comparison of K content measured by portable XRF and the declared K content for samples with independent assessments.

using the two methods used in this paper faces some challenges. Although great care is taken when cutting rock slices, there may be some variation in slice thickness, and during slicing some parts may break off. Thus the area and mass may vary from one slice to another. Furthermore, for beta counting, the standards used were powder-filled pots, which is a different geometry to our rock slice samples. Thus correction is also needed for the slices to convert the beta count rate to beta dose rate.

### 3.1. Beta counting

#### 3.1.1. Different slice thickness

When cutting slices for dating we maintain a thickness of ~0.44 mm with a tolerance of ~0.02 mm. However, to test the impact of variations in thickness upon the beta count rate, slices of different thicknesses were measured and their beta count rates compared. Fig. 2 shows the data for 3 intact slices from a homogeneous greywacke (AW-01, see Ou et al., 2018 for sample details), with thicknesses of 0.38 mm, 0.78 mm and 1.25 mm. In addition, we also measured slices cut from the Big Obsidian Flow (BOF) sample which was chosen with the aim of providing a rock that had homogeneous distribution of radionuclides (Laidley and McKay, 1971). These slices of BOF have thicknesses from 0.34 to 0.49 mm, but to measure a wider range of thicknesses we also combined two or more slices to create slices up to 1.21 mm thick (Fig. 2). As can be seen, the beta count rate increases with slice thickness, and the relationship can be fitted with a saturating exponential function. The scatter around the fit (especially visible for BOF where the greatest number of slices has been measured) is likely to reflect small scale variations in radionuclides from one slice to another (see data in section 4.1). Correcting for variations in thickness is possible, but with the exception of this experiment where variation in thickness is deliberately explored, elsewhere in this study we used slices that are as uniform in thickness as possible, and excluded slices which had different thicknesses in the same core, thus avoiding the need to correct for thickness.

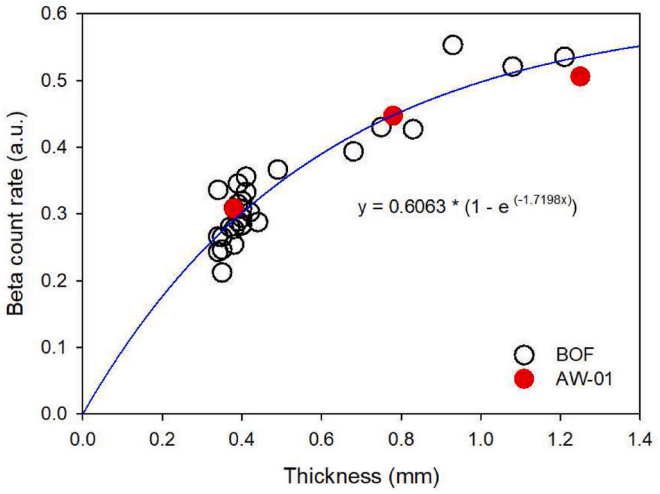


**Fig. 2.** Relationship between slice thickness and beta count rate of greywacke (AW-01) and Big Obsidian Flow sample (BOF). The beta count rate for AW-01 has been scaled by a factor of 2.2 to account for the difference in activity between the two samples. The fit is a saturating exponential.

#### 3.1.2. Broken slices

To investigate the influence of broken slices on beta count rate, three slices with the same thickness (0.41 mm) from a homogeneous greywacke AW-01 were weighed and then measured using the beta counter. The slices were then deliberately broken (roughly in half) and each fragment was weighed and measured separately in the beta counter. The fragments were then broken into smaller fragments and measured again, and so on. In this way we obtained a data set of beta count rates for slices of the same thickness, but of different mass. As can be seen from Fig. 3, the beta count rate grows linearly as a function of mass. For broken slices, the beta count rate can be corrected by the formula:

$$B_i = \frac{B_f}{0.9563\left(\frac{W_f}{W_i}\right)} \quad \text{Eq. 1}$$

where $B_i$ is corrected beta count rate as if the fragment is an 'intact' whole slice, $B_f$ is beta count rate of the fragment, $W_f$ is the weight of the fragment, and $W_i$ is the average weight of intact slices of that rock (note that this correction should be implemented for slices with the same thickness).

#### 3.1.3. Different geometry

As mentioned in Section 2.1, the standards used for beta counting (MgO and Shap granite) are powdered sample packed into pots. This is a different geometry (form, area, and thickness) to the rock slice samples. To convert the beta count rate obtained from rock slices to an infinite

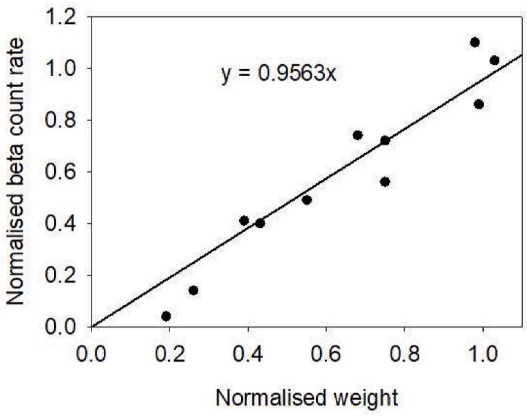


**Fig. 3.** Relationship between the mass of intact slices of uniform thickness and of their fragments, and their beta count rate of 3 slices from the greywacke sample AW-01. Both beta count rate and weight were normalised to the average value of the 3 intact slices.

matrix beta dose rate (in Gy/ka), three rock samples were chosen which showed the lowest heterogeneity in their dose rate, and a direct comparison was made between the beta dose rate obtained by crushing a sub-sample of the rock (see Section 2.1), and the average beta count rate from between 19 and 22 rock slices of each sample. The first sample was the Big Obsidian Flow (BOF), and the other two are rocks from Lydiate Lane (LL1D-01 and LL1D-04). In each case 15–20 g of the rock was milled to powder, and three replicate packed-pots (~3 g each) of the powdered sample were measured to obtain the infinite matrix beta dose rate (Gy/ka) with the same geometry as the powdered standards (Table 1). The ratio of the beta dose rate divided by the mean value of the beta count rate from the slices provides a correction factor for the difference in geometry and density (last column in Table 1). The correction factors obtained from these three different samples are consistent with each other within uncertainties, and the average value (10.61 ± 0.41) is used to convert the beta count rate from rock slices into a beta dose rate in the rest of this paper.

### 3.2. Portable XRF K content

#### 3.2.1. Different slice thickness

To test the influence of thickness variation on the results of the K content derived from the portable XRF, slices with different thicknesses (~0.4–2.4 mm) from 5 different rocks (a greywacke, a sandstone, a quartzite, and two granites) which had been previously investigated for light attenuation (Ou et al., 2018) were measured. Since XRF only probes a thin surface layer (~30 μm for K, Potts et al., 1997), it is not surprising to see (Fig. 4) that K content shows no systematic trend in K content with thickness. The variability seen in the two granites (BTH-01 and CW-01) is thought to reflect the coarser crystal size in these rocks compared with the others (Ou et al., 2018), and to reflect variation of K content between the surfaces of different slices.

#### 3.2.2. Broken slices

A total of six slices from two cobbles (AW-01 and CO-01, three slices each) were measured using the portable XRF and measured again after they were broken into smaller fragments, following the same experimental design as used in Section 3.1.2. The portable XRF measurements were made by placing the rock slices (or broken slices) on a silica substrate, and so where the rock slice only filled part of the portable XRF field-of-view (FOV, 6 mm in diameter, and 73.5% in area of our intact slice) then the remainder of the FOV will be silica, and hence a linear relationship is expected between fragment size and K content up to the point where the sample fills the FOV. Once the sample fills the FOV, any increase in sample size would not be expected to change the measured K content. Complete slices are slightly larger than the FOV, and this is the reason no further change in K content is seen for the most complete slices (Fig. 5). The K content measured with portable XRF from broken slices

**Table 1**
Assessment of the correction factor for comparing beta count rate from ~3 g powdered samples packed into pots ~25 mm in diameter and ~6 mm deep, with that from intact rock slices ~7 mm diameter and 0.44 mm thick (note that beta count from the ~0.38 mm thick BOF slices had been corrected using the relationship shown in Fig. 2 to make the data comparable with the ~0.44 mm thick slices of other cobbles).

| Sample | Infinite matrix beta dose rate from powdered sample (Gy/ka) | Beta count rate from rock slices | Number of slices counted | Ratio beta dose rate to beta count rate from rock slices |
|---|---|---|---|---|
| BOF | 3.47 ± 0.05 | 0.32 ± 0.04 | 22 | 10.73 ± 1.32 |
| LL1D-01 | 4.38 ± 0.10 | 0.43 ± 0.04 | 19 | 10.15 ± 0.99 |
| LL1D-04 | 4.33 ± 0.09 | 0.40 ± 0.04 | 20 | 10.95 ± 1.23 |

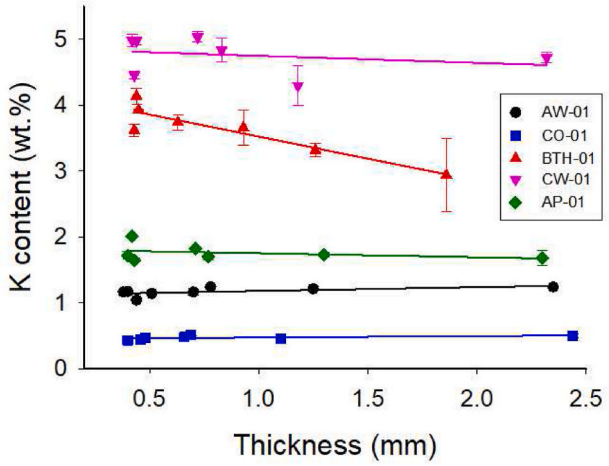


**Fig. 4.** Portable XRF K content of different thickness of slices from 5 rock types (for sample details see Ou et al., 2018). K content was measured 2–3 times for each slice. The data points represent the mean values and the error bars represent the standard deviation.

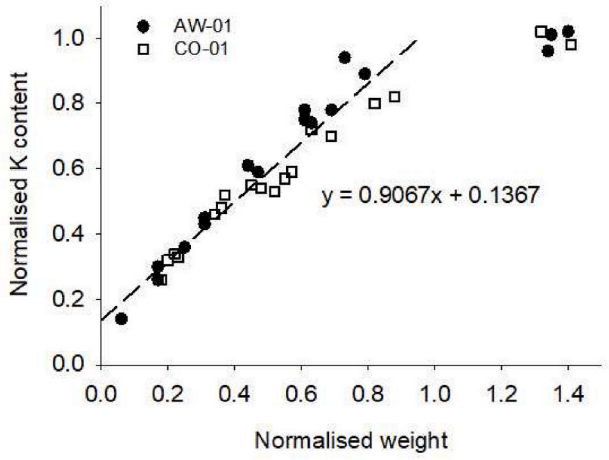


**Fig. 5.** Relationship between the weight of slices and value of K determined from portable XRF for greywacke sample AW-01 and sandstone sample CO-01. Both K content and weight were normalised to the average values of 2 or 3 intact slices for each rock sample.

can be corrected according to the formula:

$$K_m = \frac{K_f}{\left(0.9067\left(\frac{W_f}{W_m}\right) + 0.1367\right)} \quad \text{Eq. 2}$$

where $K_m$ is the K content as if the fragment is a slice with maximum analysable mass, i.e. in an area equal to the portable XRF FOV, which means 73.5% of an intact slice, $K_f$ is the measured K content of the fragment, $W_f$ is the weight of the fragment, and $W_m$ is the weight of a slice with maximum analysable mass, which means 73.5% of the average weight of intact slices. For intact slices or slices whose weight are above the maximum analysable mass, no correction is conducted. Correction should be conducted for slices from the same rock with the same thickness.

## 4. Assessing beta dose rate variability within cobbles: application to glaciofluvial samples for burial dating

Having established that the portable XRF and GM-25-5 beta counter can give quantitative assessments of the potassium content and the beta

dose rate respectively for individual rock slices, the ability of these two instruments to assess the beta dose rate variability through a rock was subsequently explored using four glaciofluvial cobbles collected for burial dating (three from Lydiate Lane (LL1D) and one from Wood Lane (WDL) in the UK). For each rock a core was drilled and slices cut from the surface to depths of between 18 and 25 mm. Care was taken to cut slices with a uniform thickness of ~0.44 mm to improve reproducibility in equivalent dose determination and to simplify the application of beta counting and the portable XRF. Prior to beta counting and portable XRF measurement, each slice was weighed (Fig. S1). This was particularly important where the slice broke during cutting or handling. For portable XRF the effect of slices breaking and only part of a slice being measured was corrected using Equation (2). For beta counting the correction in Equation (1) was applied, and the beta count rate multiplied by the value of 10.61 ± 0.41 to calculate the infinite matrix beta dose rate for each slice (as described in Section 3.1.3). The same approach was also taken for a core drilled from a piece of the Big Obsidian Flow (Laidley and McKay 1971). The slices from this rock were thinner (~0.38 mm) than those from the glaciofluvial rocks. This difference in thickness makes no impact upon the portable XRF measurements, but there is a small effect on the beta count rate, and so the relationship shown in Fig. 2 was used to make the BOF data comparable with the ~0.44 mm thick slices from the glaciofluvial samples.

### 4.1. Big Obsidian Flow

The sample from Big Obsidian Flow (BOF) was included in this study because previous analyses had demonstrated that the flow was chemically highly homogenous. Laidley and McKay (1971) took 66 samples from a transect along the 1.5 km length of the flow and 25 samples from a grid covering an area of 10 by 10 m, and found that the relative standard deviation of the concentration of $K_2O$ was at most 0.70%. Portable XRF measurements of 23 slices of BOF (Fig. 6) show that the distribution of K at this much smaller scale of analysis is also highly homogenous, with a relative standard deviation of 2.1% (Table 2). In contrast, data from beta counting shows higher variability (Fig. 6) with an RSD of 12.5% (Table 2). This RSD is significantly higher than the value of 5.9% obtained from replicate measurements (section 2.2) and implies that U and Th are less homogenous in BOF than K. It had been hoped that slices of BOF could be used as standards for beta counting to avoid the need to correct for the difference in geometry between powders and slices (section 3.1.3), but the high RSD (12.5%) observed for the beta counting data make this unfeasible. Future work will be needed to obtain a material whose radionuclides are sufficiently spatially homogeneous to make it a suitable standard for beta counting.

**Table 2**
Summary data for rock slices from Big Obsidian Flow (BOF) and four glaciofluvial samples shown in Fig. 6. K content was measured for each slice with portable XRF and the beta dose rate for each slice using the GM-25-5 beta counter.

| Sample | Average K (wt.%) | RSD K (%) | Average Beta Dose Rate (Gy/ka) | RSD Beta Dose rate (%) |
|---|---|---|---|---|
| BOF | 2.96 | 2.1 | 3.44 | 12.5 |
| LL1D-01 | 3.63 | 14.6 | 4.62 | 9.2 |
| LL1D-04 | 3.96 | 16.2 | 4.20 | 11.0 |
| LL1D-09 | 3.05 | 38.1 | 3.41 | 33.6 |
| WDL-02 | 1.26 | 26.8 | 1.74 | 36.0 |

### 4.2. Glaciofluvial cobbles

The infinite matrix beta dose rate and K content from the portable XRF of slices from the four glaciofluvial cobbles are shown as a function of depth (β-depth profile and K-depth profile, respectively) in Fig. 6. The three cobbles from Lydiate Lane have K contents (3.05 wt%-3.96 wt%) and beta dose rates (3.41–4.62 Gy/ka) consistent with other granite cobbles collected from the Isle of Man (4.5–5.2 Gy/ka, Jenkins et al., 2018), and Bridgwalton (3.9 wt% K and 4.6 Gy/ka, Chiverrell et al., 2021). In contrast, the cobble from Wood Lane has much lower K content (1.26 wt%) and beta dose rate (1.74 Gy/ka).

For the glaciofluvial cobbles, beta dose rate and K content show variation along the profiles (Fig. 6), but different cobbles show different magnitudes of variation. Some rocks are quite homogeneous, with little variation in radionuclides with depth (LL1D-01, LL1D-04), while others are more heterogeneous (LL1D-09 and WDL-02) (Table 2). Similar patterns are observed in the K content and in the beta dose rate. The K

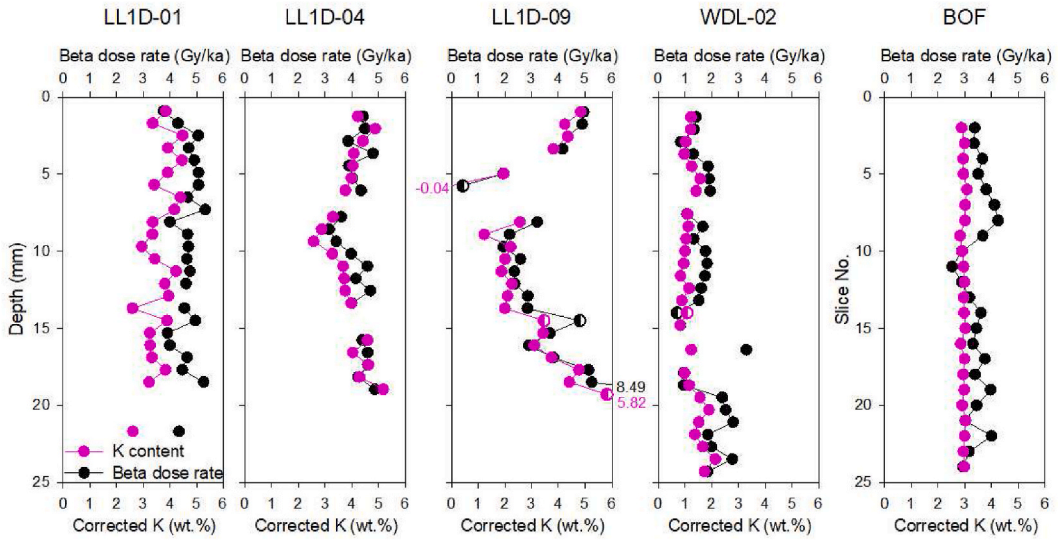


**Fig. 6.** Beta dose rate with depth (β-depth profile) and portable XRF K content (corrected for FOV) with depth (K-depth profile) of rock slices (~0.44 mm thickness) from 4 glaciofluvial granite cobbles from UK, and beta dose rate and portable XRF K content of different slices (~0.38 mm thickness) of obsidian sample BOF. Note that the y axis of LL1D-01, LL1D-04, LL1D-09, and WDL-02 is depth (mm), while for BOF slice number is shown as slices were taken from multiple cores to establish the degree of chemical homogeneity of this relatively thin sample, rather than for dating. Semi filled circles indicate slices which broke and whose mass is less than 50% of the average of intact slices.

content and beta dose rate of LL1D-09, and the beta dose rate of WDL-02 vary by more than a factor of 2 with depth. For LL1D-09, some of the data points exhibit extreme values (e.g. 5.82 wt% K and 8.49 Gy/ka beta dose rate at a depth of ~19 mm). These values are from small fragments with low mass (less than 50% of an intact fragment, and often much less than this) where individual crystals (e.g. quartz or zircons) may dominate the fragment (Fig. S1). For assessing the RSD of cobbles (Table 2), data where the mass was 50% or lower than that of an intact slice were discarded.

Our data for beta dose rate measured by beta counting, and K content measured by portable XRF, are generally well-matched. However, as demonstrated by previous studies (Ankjærgaard and Murray, 2007; Plachy and Sutton, 1982), the beta dose is mainly derived from $^{40}$K of potassium feldspar, and therefore it is not necessarily surprising that the two data sets in this study match each other. The beta dose rate from beta counting is derived from U (uranium), Th (thorium) and K from the entire slice (although there will be some bias towards the uppermost part of the slice, even for thin slices of ~0.4 mm thickness). In contrast, for portable XRF, we only measure the K content. According to analysis of andesitic, basaltic and rhyolitic samples (Potts et al., 1997), 99% of the XRF signal for K originates from the top ~ 30 μm surface layer, 50% of which originates from the top ~ 4.5 μm layer. It can be deduced that the XRF signal-derived K content for our samples likely originates from the top tens of μm and with bias to the upper surface of each slice.

Our results confirm that radionuclide heterogeneity occurs in rocks (Fang et al., 2018; Sellwood et al., 2019), and that it leads to variation of beta dose rate (Fig. 6), but without measurements such as those described in this paper it is hard to predict the degree or severity of heterogeneity. Three cobbles (LL1D-01, LL1D-04 and LL1D-09) of the same lithology (granite) and from the same site (Lydiate Lane) showed very different beta dose rate variation along their profiles. LL1D-01 and LL1D-04 are relatively homogeneous while LL1D-09 is very heterogeneous in beta dose rate distribution.

### 4.3. Assessing the likely impact of variability in the beta dose rate of individual rock slices

Samples LL1D-04 and LL1D-09 (Chiverrell et al., 2021), and WDL-02 (unpublished data) were cobbles which had been previously investigated to determine their burial age. When ages were calculated, radionuclides had been assumed to be homogenously distributed inside these cobbles, in accordance with most previous studies. For sample LL1D-04, this assumption may be valid and any variability in the age-depth profile from such a rock type should represent a genuine change in bleaching/burial history, rather than any change in dose rate influencing the age. But for sample LL1D-09 (Fig. 6), the assumption of homogeneous radionuclide distribution is not appropriate. Here, the age and thus the age-depth profile should be interpreted with caution because the beta dose rate varies so much along the profile. In this instance only the upper 5 mm of the cobble appeared to have been bleached, and no other plateaus had been described (Chiverrell et al., 2021), so the beta dose heterogeneity probably had little impact. For sample WDL-02, multiple "plateaus" appeared along the age-depth profile (unpublished data) and this had previously been thought to reveal multiple events, but the complexity of the data in Fig. 6 suggests that some of this variation is likely due to variations in beta dose rate.

Dose rate calculations for rock slices from cobbles have commonly assumed that radionuclides in the cobble are homogeneously distributed, and the beta dose rate arising from the cobble itself only varies as one approaches the surface of the cobble where the beta dose rate from the surrounding sediment may be different (e.g. Fig. 2 in Freiesleben et al., 2015). Riedesel and Autzen (2020) have recently recalculated the attenuation coefficient for beta particles in rocks and suggested that the value is approximately double the value previously used. The implication of this is that spatial variations in beta dose rate along a core will not be smoothed out as much as previously thought. Infinite matrix beta dose rate is achieved at ~1.5 mm into the rock (Riedesel and Autzen, 2020), and at 0.4 mm depth into the rock ~ 75% of the infinite matrix dose rate is reached. We have modelled the impact of adjacent rock slices of different beta activities (as seen in Fig. 6) using the new beta attenuation coefficients of Riedesel and Autzen (2020) to see what the beta dose rate received by each slice would be. For slices from these 4 glaciofluvial cobbles (~0.44 mm thick and with ~0.3 mm rock ground away during cutting of each slice), the impact of beta activity from one slice upon adjacent slices is small. Typically the modelled beta dose rate is within 5% or less of the beta dose rate measured for each slice using the beta counter. The same argument would apply to any changes in radionuclide concentration that occurred laterally (i.e. at right angles to the direction in which the core was drilled), and these would be expected to have little impact on beta dose rate.

## 5. Discussion

This study demonstrates that both beta counting and portable XRF are effective tools for rapid assessment of beta dose variation inside rocks using the approaches described here. There are two advantages for these approaches as compared to other methods such as micro XRF, SEM, QEM-EDS, and LA-ICP-MS (e.g. Fang et al., 2018; Sellwood et al., 2019). Firstly, only relatively inexpensive equipment is required for both beta counting and portable XRF methods, thus making them practical in most Geoscience or luminescence laboratories. Secondly, measurements are rapid. For beta counting 3 slices can be measured in about 24 h, while for portable XRF analysis for each slice is only for 35 s meaning that within an hour it is possible to determine K for slices from an entire rock core. Although portable XRF is obviously much faster than beta counting, beta counting provides a more complete measurement, involving emission from the whole slice, and including the contribution from U and Th as well as K.

There are some limitations for the use of beta counting and portable XRF measurements to assess beta dose rate variability. Firstly, both beta counting and portable XRF provide an indication of the beta dose variability between the slices measured through a core, but unlike methods such as micro XRF, SEM, QEM-EDS, and LA-ICP-MS cannot provide any information on the spatial variability across an individual rock slice. However, where luminescence is measured from the whole slice (e.g. Freiesleben et al., 2015; Jenkins et al., 2018; Souza et al., 2019) then using the average beta dose rate determined for the whole slice is appropriate.

Secondly, the detection limit of the portable XRF makes assessment of U and Th content challenging, and hence we focused upon the acquisition of data relating to K content. In situations where K was consistent, but U and Th varied (e.g. BOF, Fig. 6) then the portable XRF alone would not be reliable in assessing whether the dose rate of a particular cobble was heterogeneous or not. According to previous studies, heterogeneous distribution of U and Th is not uncommon in rock samples, and the presence of hot spots of U or Th will have a great impact on dose rate (Fang et al., 2018); this has also been reported for sediments (Jankowski and Jacobs, 2018). However, it may be more common that there is a relationship between total beta activity and K content (e.g. Fig. 7) in which case the portable XRF could provide a rapid means of assessing the likely beta dose rate variability. Obtaining U and Th values using portable XRF may be feasible, but will require longer measurement times due to the low concentrations and will likely have relatively large measurement uncertainties; further work is needed to explore this.

Thirdly, the accuracy of radionuclide concentrations from portable XRF is less than some other geochemical techniques. Furthermore, using portable XRF the detected signal of K content arises from only the top of a slice, and hence will not be representative of the whole slice if the sample is compositionally anisotropic. Nevertheless, our study illustrates that portable XRF is adequate for rapidly assessing beta dose rate variation and hence potentially screening samples prior to further, more

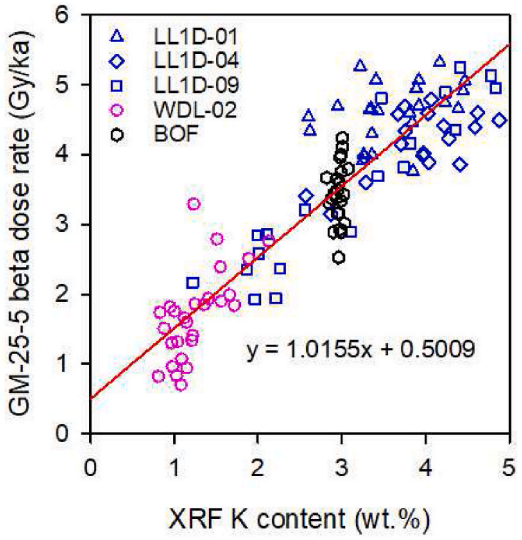


**Fig. 7.** Data from Fig. 6 shown as a bivariate plot to display the relationship between the K content derived from XRF and the beta dose calculated from beta counting.

time-consuming measurements being considered.

Where equivalent dose ($D_e$) values have already been determined for rock slices, such rapid assessment of the likely dose rate could be combined with the $D_e$ values for the same slices to give an approximation of the likely ages of each slice. However, for more precise calculation of the final age of each slice, beta counting and/or full geochemical analysis and modelling of beta dose rate is needed.

The methods introduced in this study can be used in two ways. Firstly they are useful for screening cobbles to assess their homogeneity before dating, thus informing decisions regarding the next steps for that sample – either to confirm sample homogeneity and hence that using an average dose rate for all slices should be acceptable for dating; or, to reject that particular cobble on the basis of sample heterogeneity; or to confirm the need for more careful consideration of the dose rate where samples are shown to be heterogeneous in nature and the sample is to be used for dating. The second way in which these methods are used is in the situation where heterogeneous rocks are identified and detailed beta dose measurements are needed to allow modelling of the dose rate to each slice. In such cases the beta counter offers a means of rapid beta dose rate assessment for each individual slice.

## 6. Conclusions

This study highlights the importance of assessment of beta dose variation for rock surface luminescence dating, not just for achieving more accurate exposure and burial age, but also for bringing two major advantages (assessment of bleaching, revealing multiple events by luminescence-depth profile) of burial dating into effect, and hence to improve our understanding of the exposure history of cobbles.

Two independent methods (beta counting and portable XRF) were used to assess dose rate variation along cores obtained from cobbles and β-depth profiles and K-depth profiles were established. For the four glaciofluvial cobbles examined, beta dose rates were seen to vary along the cores, and the degree of variability differs between cobbles even for a single lithology at a single site. For the investigated cobbles, the beta dose rate has been shown to vary by over a factor of two along the profile. As beta dose rate dominates the total dose rate of many rock samples, its variation will have a great impact on rock surface luminescence dating for both determining the exposure and burial age of rocks. It can be deduced that not every variation in equivalent dose or the $L_n/T_n$ ratio through a rock is due to bleaching events. Beta dose variability within the rock cannot be ignored in rock surface luminescence dating, and should routinely be considered.

Both beta counting and portable XRF are practical and rapid methods which can be used as routine methods to assess beta dose rate variation. Portable XRF is much faster than beta counting, although this provides information on K content only; nevertheless portable XRF could be used for rapid assessment of likely dose rate homogeneity/heterogeneity for screening purposes of the vast majority of geological materials. Beta counting is slower compared to portable XRF measurements; nevertheless, beta counting is still capable of providing relatively rapid assessments of dose rate variability, and offers the advantage of directly measuring the beta dose rate which can be used subsequently for the further determination of age for individual slices, and modelled across rock cores to assess the veracity of plateaus in final down-core age determinations.

The beta dose rate or K content of fragments of slices can be corrected to whole-slice equivalent diameters. However, it is recommended that slices should be as uniform in thickness as possible, and as intact as possible, because correction for heterogeneous rocks may otherwise be a challenge.

For rock surface luminescence dating, it has hitherto been largely assumed that the rocks used for dating have homogeneous radionuclide distributions. If this were not to be the case, unaccounted for variability in the dose rate through a rock profile may conceivably cause variations in the age-depth profile which could potentially be misinterpreted as previous exposure/deposition events. Caution should be paid when calculating the age and identifying different events by 'plateaus' in the luminescence-depth profiles. To correctly interpret such depth profiles, it may be necessary to measure and model the beta dose rate for every single rock slice for these rocks to distinguish between multiple exposure events and the impact of dose rate inhomogeneity. The portable XRF allows rapid screening of likely inhomogeneity, and beta counting allows relatively straightforward and inexpensive measurement of the beta dose rate for individual rock slices suitable for such assessments.

## Declaration of competing interest

The authors declare that they have no known competing financial interests or personal relationships that could have appeared to influence the work reported in this paper.

## Acknowledgements

XJO thanks support from the National Natural Sciences Foundation of China (grants 42071088). This work was funded by the European Union's Horizon 2020 research and innovation programme under the Marie Skłodowska-Curie grant agreement No 663830. Richard Chiverrell helped sampling in the field for the UK sites. Nick Pearce kindly provided the Big Obsidian Flow sample. Ian Saunders, Tommy Ridgway, Geraint Jenkins, Svenja Riedesel, and Hollie Wynne are appreciated for their assistance in the laboratory. Research in Next Generation Luminescence methods in Aberystwyth is supported by NERC grant CC003, and by HEFCW infrastructure funding for SPARCL. Two anonymous referees are thanked for their comments which helped to improve this paper.

## Appendix A. Supplementary data

Supplementary data to this article can be found online at https://doi.org/10.1016/j.quageo.2022.101349.

## References

Ageby, L., Angelucci, D.E., Brill, D., Carrer, F., Rades, E.F., Rethemeyer, J., Brückner, H., Klasen, N., 2021. Rock surface IRSL dating of buried cobbles from an alpine dry-stone structure in Val di Sole, Italy. Quat. Geochronol. 66, 101212.

al Khasawneh, S., Murray, A., Abudanah, F., 2019. A first radiometric chronology for the Khatt Shebib megalithic structure in Jordan using the luminescence dating of rock surfaces. Quat. Geochronol. 49, 205–210.
Ankjaergaard, C., Murray, A.S., 2007. Total beta and gamma dose rates in trapped charge dating based on beta counting. Radiat. Meas. 42, 352–359.
Bailiff, I.K., Bridgland, D., Cunha, P.P., 2021. Extending range of OSL dating using vein-quartz and quartzite sedimentary pebbles. Quat. Geochronol. 65, 101180.
Bøtter-Jensen, L., Mejdahl, V., 1988. Assessment of beta dose-rate using a GM multicounter system. Nucl. Tracks Radiat. Meas. 14, 187–191.
Brill, D., May, S.M., Mhammdi, N., King, G., Lehmann, B., Burow, C., Wolf, D., Zander, A., Bruckner, H., 2021. Evaluating optically stimulated luminescence rock surface exposure dating as a novel approach for reconstructing coastal boulder movement on decadal to centennial timescales. Earth Surf. Dyn. 9, 205–234.
Chiverrell, R.C., Thomas, G.S.P., Burke, M., Medialdea, A., Smedley, R., Bateman, M., Clark, C., Duller, G.A.T., Jenkins, G., Ou, X., Roberts, H.M., Scourse, J., 2021. The evolution of the terrestrial - terminating Irish Sea glacier during the last glaciation. J. Quat. Sci. 36, 752–779.
De Corte, F., Vandenberghe, D., Hossain, S.M., De Wispelaere, A., Buylaert, J.-P., Van den Haute, P., 2007. Preparation and characterization of loess sediment for use as a reference material in the annual radiation dose determination for luminescence dating. J. Radioanal. Nucl. Chem. 272, 311–319.
Fang, F., Martin, L., Williams, I.S., Brink, F., Mercier, N., Grün, R., 2018. 2D modelling: a Monte Carlo approach for assessing heterogeneous beta dose rates in luminescence and ESR dating: paper II, application to igneous rocks. Quat. Geochronol. 48, 195–206.
Feathers, J., More, G.M., Quinteros, P.S., Burkholder, J.E., 2019. IRSL Dating of rocks and sediments from desert geoglyphs in coastal Peru. Quat. Geochronol. 49, 177–183.
Freiesleben, T., Sohbati, R., Murray, A., Jain, M., Khasawneh, S.A., Hvidt, S., Bo, J., 2015. Mathematical model quantifies multiple daylight exposure and burial events for rock surfaces using luminescence dating. Radiat. Meas. 81, 16–22.
Gliganic, L.A., Meyer, M.C., May, J.-H., Aldenderfer, M.S., Tropper, P., 2021. Direct dating of lithic surface artifacts using luminescence. Sci. Adv. 7, eabb3424.
Higgins, M.W., 1973. Petrology of Newberry volcano, central Oregon. Geol. Soc. Am. Bull. 84, 455–488.
Ishii, Y., Takahashi, T., Ito, K., 2022. Luminescence dating of cobbles from Pleistocene fluvial terrace deposits of the Ara River, Japan. Quat. Geochronol. 67, 101228.
Jankowski, N.R., Jacobs, Z., 2018. Beta dose variability and its spatial contextualisation in samples used for optical dating: an empirical approach to examining beta microdosimetry. Quat. Geochronol. 44, 23–37.
Jenkins, G.T.H., Duller, G.A.T., Roberts, H.M., Chiverrell, R.C., Glasser, N.F., 2018. A new approach for luminescence dating glaciofluvial deposits - high precision optical dating of cobbles. Quat. Sci. Rev. 192, 263–273.
Laidley, R.A., McKay, D.S., 1971. Geochemical examination of obsidians from Newberry Caldera, Oregon. Contrib. Mineral. Petrol. 30, 336–342.
Lehmann, B., Valla, P.G., King, G.E., Herman, F., 2018. Investigation of OSL surface exposure dating to reconstruct post-LIA glacier fluctuation in the French Alps (Mer de Glace, Mont-Blanc massif). Quat. Geochronol. 44, 63–74.
Liritzis, I., 2011. Surface dating by luminescence: an overview. Geochron 38, 292–302.
Luo, M., Chen, J., Liu, J., Qin, J., Owen, L.A., Han, F., Yang, H., Wang, H., Zhang, B., Yin, J., Li, Y., 2018. A test of rock surface luminescence dating using glaciofluvial boulders from the Chinese Pamir. Radiat. Meas. 120, 290–297.
Murray, A., Buylaert, J.-P., Thiel, C., 2015. A luminescence dating intercomparison based on a Danish beach-ridge sand. Radiat. Meas. 81, 32–38.
Ou, X.J., Roberts, H.M., Duller, G.A.T., Gunn, M.D., Perkins, W.T., 2018. Attenuation of light in different rock types and implications for rock surface luminescence dating. Radiat. Meas. 120, 305–311.
Plachy, A., Sutton, S., 1982. Determination of the dose-rate to quartz in granite. PACT 6, 188–194.
Potts, P.J., Williams-Thorpe, O., Webb, P.C., 1997. The bulk analysis of silicate rocks by portable X-Ray fluorescence: effect of sample mineralogy in relation to the size of the excited volume. Geostand. Newsl. 21, 29–41.
Rades, E., Sohbati, R., Lüthgens, C., Jain, M., Murray, A., 2018. First luminescence depth profiles from boulders from moraine deposits: insights into glaciation chronology and transport dynamics in Malta valley, Austria. Radiat. Meas. 120, 281–289.
Riedesel, S., Autzen, M., 2020. Beta and gamma dose rate attenuation in rocks and sediment. Radiat. Meas. 133, 106295.
Sellwood, E.L., Guralnik, B., Kook, M., Prasad, A.K., Sohbati, R., Hippe, K., Wallinga, J., Jain, M., 2019. Optical bleaching front in bedrock revealed by spatially-resolved infrared photoluminescence. Sci. Rep. 9, 1–12.
Simkins, L.M., DeWitt, R., Simms, A.R., Briggs, S., Shapiro, R.S., 2016. Investigation of optically stimulated luminescence behavior of quartz from crystalline rock surfaces: a look forward. Quat. Geochronol. 36, 161–173.
Sohbati, R., Liu, J., Jain, M., Egholm, D., Paris, R., Guralnik, B., 2018. Centennial-to millennia-scale hard rock erosion rates deduced from luminescence-depth profiles. Earth Planet Sci. Lett. 493, 218–230.
Sohbati, R., Murray, A.S., Jain, M., Buylaert, J.-P., Thomsen, K., 2011. Investigating the resetting of OSL signals in rock surfaces. Geochronometria 38 (3), 249–258.
Sohbati, R., Murray, A.S., Porat, N., Jain, M., Avner, U., 2015. Age of a prehistoric "Rodedian" cult site constrained by sediment and rock surface luminescence dating techniques. Quat. Geochronol. 30, 90–99.
Souza, P.E., Sohbati, R., Murray, A.S., Kroon, A., Clemmensen, L.B., Hede, M.U., Nielsen, L., 2019. Luminescence dating of buried cobble surfaces from sandy beach ridges: a case study from Denmark. Boreas 48, 841–855.